







Article

In Vitro Alpha-Glucosidase and Alpha-Amylase Inhibitory Activities and Antioxidant Capacity of *Helichrysum cymosum* and *Helichrysum pandurifolium* Schrank Constituents

Baraa M. I. S. Jadalla ¹, Justin J. Moser ², Rajan Sharma ^{2,*}, Ninon G. E. R. Etsassala ³, Samuel Ayodele Egieyeh ¹, Jelili A. Badmus ⁴, Jeanine L. Marnewick ⁴, Denzil Beukes ², Christopher N. Cupido ⁵ and Ahmed A. Hussein ^{2,*}

¹ School of Pharmacy, University of the Western Cape, Symphony Rd., Bellville 7535, South Africa; 3876610@myuwc.ac.za (B.M.I.S.J.); segieyeh@uwc.ac.za (S.A.E.)

² Chemistry Department, Cape Peninsula University of Technology, Bellville Campus, Symphony Road, Bellville 7535, South Africa; jmoser1.618@gmail.com (J.J.M.); dbeukes@uwc.ac.za (D.B.)

³ Department of Horticultural Sciences, Cape Peninsula University of Technology, Symphony Rd., Bellville 7535, South Africa; etsassalan@cput.ac.za

⁴ Applied Microbial and Health Biotechnology Institute, Cape Peninsula University of Technology, Symphony Rd., Bellville 7535, South Africa; jabadmus@lautech.edu.ng (J.A.B.); marnewickj@cput.ac.za (J.L.M.)

⁵ Department of Botany, University of Fort Hare, Private Bag X1314, Alice 5700, South Africa; ccupido@ufh.ac.za

* Correspondence: sharmar@cput.ac.za (R.S.); mohammedam@cput.ac.za (A.A.H.)



Citation: Jadalla, B.M.I.S.; Moser, J.J.; Sharma, R.; Etsassala, N.G.E.R.; Egieyeh, S.A.; Badmus, J.A.; Marnewick, J.L.; Beukes, D.; Cupido, C.N.; Hussein, A.A. In Vitro Alpha-Glucosidase and Alpha-Amylase Inhibitory Activities and Antioxidant Capacity of *Helichrysum cymosum* and *Helichrysum pandurifolium* Schrank Constituents. *Separations* **2022**, *9*, 190. <https://doi.org/10.3390/separations9080190>

Academic Editor: Kazuya Murata

Received: 30 April 2022

Accepted: 11 June 2022

Published: 26 July 2022

Publisher's Note: MDPI stays neutral with regard to jurisdictional claims in published maps and institutional affiliations.



Copyright: © 2022 by the authors. Licensee MDPI, Basel, Switzerland. This article is an open access article distributed under the terms and conditions of the Creative Commons Attribution (CC BY) license (<https://creativecommons.org/licenses/by/4.0/>).

Abstract: Diabetes mellitus (DM) is a group of systemic metabolic disorders with a high rate of morbidity and mortality worldwide. Due to the detrimental side effects of the current treatment, there is a great need to develop more effective antidiabetic drugs with fewer side effects. Natural products are a well-known source for the discovery of new scaffolds for drug discovery, including new antidiabetic drugs. The genus *Helichrysum* has been shown to produce antidiabetic natural products. In this investigation, the methanolic extract of *H. cymosum* and *H. pandurifolium* resulted in the isolation and identification of eleven known compounds viz 5,8-dihydroxy-7-methoxy-2-phenyl flavanone (**1**), pinostrobin (**2**), dihydrobaicalein (**3**), glabranin (**4**), allopaturetin (**5**), pinostrobin chalcone (**6**), helichrysetin (**7**), 5-hydroxy-3,7-dimethoxyflavone (**8**), 3,5-dihydroxy-6,7,8-trimethoxyflavone (**9**), 3-O-methylquercetin (**10**), and 3-methylethergalangin (**11**). The in vitro bio-evaluation of isolated compounds against alpha-glucosidase showed that **10**, **5**, and **11** demonstrated the highest alpha-glucosidase inhibitory activity with IC₅₀ values of 9.24 ± 0.4, 12.94 ± 0.2, and 16.00 ± 2.4 µM respectively, followed by **7** and **3** with IC₅₀ values of 18.16 ± 1.2 and 44.44 ± 0.2 µM respectively. However, none of these compounds showed a measurable inhibitory effect on alpha-amylase under the experimental conditions used except compound **10** which showed a poor alpha-amylase inhibitory activity with an IC₅₀ value of 230.66 ± 15.8 µM. Additionally, strong total antioxidant capacities were demonstrated by **10**, **5** and **7** in ferric-ion reducing antioxidant power assay (374.34 ± 69.7; 334.37 ± 1.7; 279.93 ± 0.8) µmol AAE/mmol. This is the first scientific report to be carried out on alpha-glucosidase inhibitory activities and antioxidant capacities of *H. cymosum* constituents and a first report on the isolation and identification of methoxyflavonoids from *H. pandurifolium*. Our findings suggest that these compounds are promising candidates to inhibit alpha-glucosidase as well as oxidative stress related to diabetes. Results from molecular docking provided insight into the observed in vitro alpha-glucosidase inhibitory activities for **5**, **7**, **10**, and **11**. It is envisaged that the isolated phytochemicals from these plants may contribute to the development of hypoglycemic lead compounds with anti-diabetic potential.

Keywords: alpha-glucosidase; Asteraceae; diabetes mellitus; flavonoids; oxidative stress

1. Introduction

Diabetes mellitus (DM), a metabolic disorder associated with chronic hyperglycemia, is one of the fastest-growing metabolic diseases today [1,2]. In 2017, it was estimated that 451 million people were living with diabetes and an estimated 850 billion US dollar global healthcare expenditure was spent on diabetes. It is estimated that a total of 693 million people could be living with diabetes by 2045 [3]. Hyperglycemia is the main consequence of DM, which results from a shortage in insulin secretion or degradation of insulin-producing beta cells of the pancreas [4]. The chronic hyperglycemia of diabetes may result in long-term damage, dysfunction, and failure of some organs, such as the eyes, kidneys, nerves, heart, and blood vessels. Many factors (internal and external) such as oxidative stress, obesity, and sedentary lifestyle are directly implicated in these cell alterations [5,6]. Inhibition of α -glucosidase and α -amylase activity is one of the therapeutic approaches being investigated for diabetes treatment. Natural products have become an increasingly popular source of hypoglycemic agents due to the high cost and common side effects of many anti-diabetic drugs [7]. Phytochemicals from plant-derived sources, such as flavonoids, have been commonly reported to inhibit digestive enzymes α -glucosidase and α -amylase enzymes [8–10]. The structure-activity relationship (SAR) between flavonoids and α -glucosidase/ α -amylase enzymes has been well documented by the scientific community [11–13].

The genus *Helichrysum* Mill. belongs to the Asteraceae family, consisting of roughly 600 different species, of which at least 250 species are found in South Africa [14]. Today, the native amaXhosa and isiZulu communities in South Africa still use *Helichrysum* for medicinal purposes [15]. *Helichrysum* is used to treat a variety of different diseases and disorders including diarrhea, gastrointestinal tract infections, cold, cough, other respiratory conditions, and skin infections [14,16].

Helichrysum cymosum (Figure 1A) is traditionally used to treat colds, coughs, fever, headaches, and wounds [17,18]. Other ethnomedicinal uses of *H. cymosum* include pertussis, influenza, treatment of blocked nose, pulmonary problems, flatulence, diarrhea, improve appetite, laxative, vomiting, dizziness, insomnia, boosting the immune system, skin infections, varicose veins, weak bones, menstrual pain, insect repellent, cardiovascular problems, kidney problems, urinary problems, and eye problems [17]. The leaves, stems, and twigs of *H. cymosum* are sold as herbal medicines in the informal herbal medicine markets in the Gauteng and the Western Cape provinces in South Africa [18]. Numerous compounds have been isolated from the alcoholic extract of the leaves and roots of *H. cymosum* including different sesquiterpenes and chalcones [19–21]. The biological investigation of *H. cymosum* extract revealed that it possesses antioxidant, antiviral, anti-HIV, anti-inflammatory, antifungal, antimalarial, antimicrobial, and cytotoxicity activities [14].

Traditionally, *H. pandurifolium* (Figure 1B) is used to treat respiratory conditions, heart troubles, constipation, back pain, and kidney stones [14]. Biological activity of *H. pandurifolium* total extract using chloroform:methanol (1:1) has been previously tested for antibacterial activity and cytotoxicity [22]. Currently, there are no reports of anti-diabetic or antioxidant studies on this species or any of its isolated compounds. Although *H. pandurifolium* finds many uses traditionally, it is a relatively understudied species of the *Helichrysum* genus [23].

As a part of a study to explore *Helichrysum* plants for hypoglycemic agents in our lab, the methanolic extracts of *H. cymosum* and *H. pandurifolium* exhibited activity against the alpha-glucosidase enzyme. In a quest to identify the active phytochemical constituents, the phytochemical analysis of these plants was undertaken. The chemical structure identification of the isolated phytochemical constituents from these plants was performed and isolated constituents were biologically evaluated for in vitro enzyme inhibitory effects on key digestive enzymes α -glucosidase and α -amylase in addition to their evaluation of their antioxidant properties by Ferric-ion Reducing Antioxidant Power (FRAP) and Trolox Equivalent Absorbance Capacity (TEAC) antioxidant assays. Molecular docking was used to explain the observed inhibitory activities as previously done for isolated constituents from *Plectranthus ecklonii* [24].

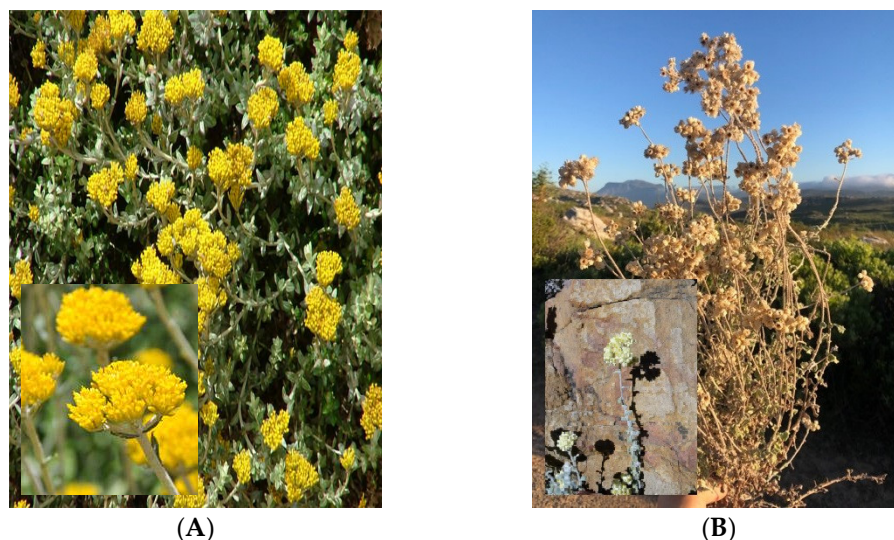


Figure 1. Photographs of *H. cymosum* (A) and *H. pandurifolium* (B) (SANBI; <http://pza.sanbi.org>, accessed on 7 April 2022).

2. Materials and Methods

2.1. Reagents

EGCG (Epigallocatechin gallate), trolox (6-hydroxyl-2, 5, 7, 8-tetramethylchroman-2-carboxylic acid), and other reagents including ABTS (2,2'-azino-bis(3-ethylbenzothiazoline-6-sulfonic acid)), potassium peroxodisulphate ($K_2S_2O_8$), perchloric acid, TPTZ (tripyrindyl triazine), iron (III) chloride hexahydrate, copper sulfate, hydrogen peroxide, alpha-glucosidase (*Saccharomyces cerevisiae*) and alpha-glucosidase (procaine pancreas), *p*-nitro-phenyl- α -D-glucopyranoside (p-NPG), 3,5-dinitro salicylic acid (DNS), Sodium carbonate, hydrochloric acid, acetic acid, sodium acetate, sodium dihydrogen phosphate, di-sodium hydrogen phosphate were obtained from Sigma-Aldrich or Merck. The organic solvents were supplied by Merck, Johannesburg, South Africa. For thin-layer chromatography, silica gel 60 H (0.040–0.063 mm particle size, Merck, South Africa) and Sephadex LH-20 (Sigma-Aldrich, Johannesburg, South Africa) were used as the stationary phase.

Nuclear magnetic resonance (NMR) spectra were recorded on Bruker 400 MHz instrument. The chemical shifts were reported as δ values in ppm downfield from tetramethylsilane (TMS) and deuterated residual peaks were used as internal standards. Absorbance values on 96-well plates were measured in clear 96-well microplates (Greiner, height 14.8 mm) using a UV plate reader (Molecular Devices Spectra Max i3X).

2.2. Collection and Identification of the Plant Material

The wild-growing *H. pandurifolium* was collected from the Cape Point Nature Reserve in Cape Town, South Africa in December 2017 whereas the aerial part of *H. cymosum* species was collected in January 2018, from Hout Bay, Cape Town, South Africa. The voucher specimens (*Helichrysum cymosum*- UFH 2020-10-02 and *Helichrysum pandurifolium*- UFH 2020-10-04) were identified by Prof. Christopher Cupido and deposited at the Department of Botany, University of Fort Hare, South Africa.

2.3. Extraction and Fractionation of the Total Extract

2.3.1. *Helichrysum cymosum*

The dried aerial parts of *Helichrysum cymosum* (330 g) were blended and extracted with methanol (2.5 L) at room temperature (25 °C) for 24 h. The methanol extract was filtered and evaporated to dryness under reduced pressure at 40 °C to yield 45.2 g. The total extract (45 g) was applied to a silica gel column (30 × 18 cm) and eluted using a gradient of Hexane/EtOAc in the order of increasing polarity. Fifty-two fractions were collected and combined according to their TLC profiles to yield twelve main fractions la-

beled I–XII. Main fraction XI (2.7 g) was subjected to silica gel column using Hexane/EtOAc gradient (7:3 and 100% EtOAc), then to Sephadex (using 90% aqueous ethanol) to produce 5,8-dihydroxy-7-methoxy-2-phenyl flavanone (**1**, 44.1 mg). The sub-fraction XI–XIV (187 mg) was subjected to Sephadex using 90% aqueous ethanol to yield pinostrobin (**2**, 21.1 mg). The sub-fraction VII (628 mg) was subjected to Sephadex (using 90% aqueous ethanol) to produce dihydrobaicalein (**3**, 14.1 mg) and glabranin (**4**, 24.1 mg). The sub-fractions VIII (253.1 mg) subjected through Sephadex using 95% aqueous ethanol produced allopaturetin (**5**, 21.1 mg). The fraction IX (230 mg) was subjected to silica gel using Hexane:EtOAc gradient (7:3 and 100% EtOAc), then preparative TLC to yield pinostrobin chalcone (**6**, 13.1 mg) and helichrysetin (**7**, 14.1 mg).

2.3.2. *Helichrysum pandurifolium*

The aerial parts (leaves and flowers) of *H. pandurifolium* (374.5 g) were extracted with methanol as previously stated. The total extract (42.2 g) was subjected to flash column chromatography using silica gel 60 H (height 70 cm, radius 5.5 cm, 6.6 L volume) and eluted using a gradient elution of hexane, ethyl acetate, and methanol. A total of fifty fractions were collected and combined according to observations after TLC plate analysis, resulting in twelve main fractions. Main fraction III (4.0 g) was subjected to a medium-sized silica gel column (90 × 2.5 cm, 1.76 L volume) and separated using a gradient elution of hexane and ethyl acetate, resulting in twelve subfractions. The main fraction IV (5.9 g) was subjected to the same conditions and resulting in twenty-four subfractions. Compound **9** (100 mg) was obtained via crystallization using methanol. The main fraction VI (8.17 g) was subjected to the same conditions followed by Sephadex LH-20 using 5.0 aqueous methanol to yield compounds **10** (132 mg). Compound **11** (20 mg) was purified from fraction VI using preparative TLC.

2.4. Structure Elucidation and Identification of the Isolated Compounds

All the isolated compounds were elucidated by NMR spectroscopy. ^1H , ^{13}C , and distortionless enhancement of polarization transfer (DEPT) analysis were performed for structural elucidation. The carbon peaks in the ^{13}C NMR spectroscopy were further differentiated as $-\text{CH}_3$, CH, or CH_2 carbons by DEPT-135 analysis. The NMR data of the compounds was compared to that available in the literature for the final identification of the compounds.

5,8-dihydroxy-7-methoxy-2-phenyl flavanone (**1**): ^1H NMR (400 MHz, CDCl_3): 11.86 (1H, s, 5-OH), 7.42 (5H, m, H-2'. H-3', H-4', H-5', H-6'), 6.06 (1H, s, H-6), 5.44 (1H, dd, $J = 1.9, 12.7$ Hz, H-2), 3.79 (3H, s), 3.05 (1H, q, $J = 4.4$ Hz each, *trans*), 2.82 (1H, dd, $J = 2.7, 17.2$ Hz, H-3 *cis*). ^{13}C NMR (100 MHz): 184.0 (C-4), 165.7 (C-2), 159.8 (C-5), 154.9 (C-8), 154.0 (C-9), 133.0 (C-4), 132.5 (C-1), 130.2 (C-7), 127.4 (C-3, 5), 126.4 (C-2, 6), 105.7 (C-10), 105.5 (C-3), 95.6 (C-6), 60.9 (C-11).

Pinostrobin (**2**): ^1H NMR (400 MHz, CDCl_3): 7.30 (5H, m, H-2'. H-3', H-4', H-5', H-6'), 5.95 (2H, d, $J = 2.72$ Hz, H-6, H-8), 5.26 (1H, dd, $J = 12.8, 2.8$ Hz, H-2), 3.72 (3H, s, 7-OMe), 3.08 (1H, dd, $J = 15.1, 12.8$ Hz, H-3 β), 2.63 (1H, dd, $J = 14.7, 2.8$ Hz, H-3 α). ^{13}C NMR (100 MHz): 190.3/C-4, 165.1/C-7, 164.8/C-9, 162.7/C-5, 138.3/C-1', 128.6/C-4', 125.9/C-2', C-3', C-5', C-6', 104.7/C-10, 96.2/C-6, 93.3/C-8, 78.8/C-2, and 55.6/C-7OMe, 45.2/C-3.

Dihydrobaicalein (**3**): ^1H NMR (400 MHz, CDCl_3): 11.93 (1H, s, 5-OH), 7.46 (5H, m, H-2'. H-3', H-4', H-5', H-6'), 6.58 (1H, s, H-8), 6.18 (1H, s, H-2), 3.90 (2H, s, H-3 $\alpha\beta$). ^{13}C NMR (100 MHz): δ 196.8/C-4, 154.8/C-7, 153.4/C-9, 150.1/C-5, 138.0/C-1', 128.4/C-4', 128.2/C-6, 128.1/C-3', 5', 126.4/C-2', 6', 103.8/C-10, 96.2/C-8, 79.8/C-2, 42.6/C-3.

Glabranin (**4**): ^1H NMR (400 MHz, CDCl_3): 12.18 (1H, s, 5-OH), 7.40 (5H, br.s), 5.96 (1H, s, H-6), 5.19 (1H, br.t, $J = 7.1$ Hz, =CH), 3.23 (2H, br. d, $J = 7$ Hz, Ar- CH_2), 3.02 (1H, dd, $J = 12.0$ and 17.5 Hz), 2.73 (1H, dd, $J = 4.5$ and 17.5 Hz), 1.70 (6H, br.s, =C(CH_3) $_2$). ^{13}C NMR (100 MHz): δ 195.6/C-4, 164.4/C-7, 160.8/C-5, 138.5/C-2'', 138.4/C-1', 129.0/C-4', 126.5/C-3', 5', 126.1/C-2', 6', 122.3/C-3'', 108.8/C-8, 102.3/C-10, 94.8/C-6, 77.4/C-2, 43.2/C-3, 27.7/C-5'', 20.1/C-1'', 17.6/C-4''.

Allopatuletin (5): ^1H NMR (400 MHz, CDCl_3): 7.63 (1H, d, $J = 2.1$ Hz, H-1'), 7.53 (1H, dd, $J = 2.1, 8.5$ Hz, H-5'), 6.91 (1H, d, $J = 8.5$ Hz, H-6'), 6.23 (1H, s, H-8), 3.74 (3H, s). ^{13}C NMR (100 MHz): δ 178.7/C-4, 163.8/C-7, 156.4/C-5, 147.8/C-2, 144.4/C-9, 138.8/C-1', 122/C-3, 121.5/C-1', 115.2/C-5', 6', 105/C-10, 98.9/C-6, 94.0/C-8, 60.0/OMe.

Pinostrobin chalcone (6): ^1H NMR (400 MHz, CDCl_3): 7.88 (1H, d, $J = 15.5$ Hz, H-7), 7.75 (1H, d, $J = 15.5$ Hz, H-8), 7.61 (2H, d, $J = 8.6$ Hz, H-2, H-6), 6.93 (2H, d, $J = 7.0$ Hz, H-3, H-5, 8.6), 6.09 (1H, d, $J = 1.68$ Hz, H-3'), 6.02 (1H, d, $J = 2.2$ Hz, H-5'), 3.97 (3H, s, MeOH). ^{13}C NMR (100 MHz): δ 192.6/C-9, 167.6/C-4', 164.9/C-6', 163.3/C-2', 142.4/C-7, 135.5/C-1, 128.3 C-2/C6, 129.9/C-4, 128.8/C-3/C-5, 127.7/C-8, 105.7/C-1', 96.2/C-3', 91.6/C-5', 55.5 (MeOH).

Helichrysetin (7): ^1H NMR (400 MHz, CDCl_3): 7.83 (1H, d, $J = 15.5$ Hz), 7.67 (1H, d, $J = 15.5$ Hz), 7.53 (2H, d, $J = 7.0$ Hz, H-2, H-6), 7.33 (2H, d, $J = 7.0$ Hz, H-3, H-5), 7.2 (1H, m, H-4), 5.94 (1H, s, H-3'), 5.89 (1H, s, H-5'), 3.84 (3H, s, MeOH). ^{13}C NMR (100 MHz): δ 192.2/C-4, 167.6/C-6', 164.8/C-4', 163.3/C-2', 142.0 (C- β), 135.5 (C-1), 128.3 (C-2/C6), 129.9 (C-4), 128.8 (C-3/C-5), 127.7 (C- α), 105.7 (C-1'), 96.2 (C-3'), 91.6 (C-5'), 55.5 (MeOH).

5-hydroxy-3,7-dimethoxyflavone (8): ^1H NMR (400 MHz, CDCl_3) δ : 12.59 (s, 1H, 5-OH), 8.08 (dd, $J = 7.2, 3.0$ Hz, 2H, H-2', H-6'), 7.52 (t, $J = 2.8$ Hz, 3H, H-3', H-4', H-5'), 6.46 (d, $J = 2.2$ Hz, 1H, 6-H), 6.37 (d, $J = 2.2$ Hz, 1H, 8-H), 3.88 (s, 3H, 3-OCH₃), 3.87 (s, 3H, 7-OCH₃). ^{13}C NMR (100 MHz) δ : 178.9 (C=O, C-4), 165.6 (C-7), 162.1 (C-5), 156.5 (C-9), 155.9 (C-2), 139.7 (C-3), 131.0 (C-4'), 130.5 (C-1'), 128.6 (C-3', C-5'), 128.4 (C-2', C-6'), 106.2 (C-10), 98.0 (C-6), 92.2 (C-8), 60.4 (CH₃, 3-OMe), 55.9 (CH₃, 7-OMe).

3,5-dihydroxy-6,7,8-trimethoxyflavone (9): ^1H NMR (400 MHz, CDCl_3): δ 11.45 (s, 1H, 5-OH), 8.27 (d, $J = 8.0$ Hz, 2H, H-2', H-6'), 7.57-7.47 (m, 3H, H-3', H-4', H-5'), 6.81-6.73 (br, 1H, 3-OH), 4.13 (s, 3H, 8-OMe), 3.99 (s, 3H, 6-OMe), 3.96 (s, 3H, 7-OMe). ^{13}C NMR (100 MHz): δ 176.2 (C=O, C-4), 153.5 (C-7), 148.0 (C-5), 145.8 (C-2), 145.4 (C-9), 136.6 (C-3), 136.0 (C-6), 133.4 (C-8), 130.9 (C-1'), 130.6 (C-4'), 128.9 (C-3', C-5'), 127.8 (C-2', C-6'), 105.5 (C-10), 62.3 (CH₃, 7-OMe), 61.9 (CH₃, 8-OMe), 61.4 (CH₃, 6-OMe).

3',4',5,7-tetrahydroxy-3-methoxyflavone (10): ^1H NMR (400 MHz, DMSO): δ 12.70 (s, 1H, 5-OH), 7.54 (d, $J = 2.4$ Hz, 1H, H-2'), 7.44 (dd, $J = 8.4, 2$ Hz, 1H, H-6'), 6.90 (d, $J = 8.4$ Hz, 1H, H-5'), 6.41 (d, $J = 2$ Hz, 1H, H-8), 6.19 (d, $J = 2$ Hz, 1H, H-6), 3.77 (s, 3H, 3-OMe). ^{13}C NMR (100 MHz) and DEPT-135: δ 179.4 (C=O, C-4), 165.8 (C-7), 162.8 (C-5), 157.9 (C-9), 157.0 (C-2), 149.6 (C-4'), 146.2 (C-3'), 139.1 (C-3), 122.6 (C-1'), 121.9 (C-6'), 116.3 (C-2'), 116.2 (C-5'), 105.5 (C-10), 99.6 (C-6), 94.6 (C-8), 60.3 (CH₃, 3-OMe).

5,7-dihydroxy-3-methoxyflavone (11): ^1H NMR (400 MHz, $(\text{CD}_3)_2\text{CO}$): 8.09-8.06 (m, 2H, H-2', H-6'), 7.56 (m, 3H, H-3', H-4', H-5'), 6.49 (d, $J = 2$ Hz, 1H, 8-H), 6.26 (d, $J = 2$ Hz, 1H, 6-H), 3.88 (s, 3H, 3-OMe). ^{13}C NMR (100 MHz): δ 179.8 (C=O, C-4), 166.3 (C-7), 163.3 (C-5), 158.3 (C-9), 156.5 (C-2), 140.4 (C-3), 131.9 (C-4'), 129.7 (C-3', C-5'), 129.4 (C-2', C-6'), 105.9 (C-10), 100.0 (C-6), 95.0 (C-8), 60.8 (CH₃, 3-OMe).

2.5. Alpha-Glucosidase Assay

The alpha-glucosidase assay of the tested compounds (1–11) was conducted according to the slightly modified standard method [25]. Into a 96-well clear microplate, 50 μL of the α -glucosidase phosphate buffer solution (pH 6.5) was added to all wells. 10 μL of the α -glucosidase enzyme solution was added to the odd-numbered wells and 10 μL of the phosphate buffer solution was added to the even-numbered wells. To the designated control wells 20 μL of methanol (HPLC grade > 99%) was added and 20 μL of the sample stock solutions (concentration range of 1 mg/mL to 0.125 mg/mL) were added in triplicate. The plate was then incubated at 37 $^\circ\text{C}$ for 15 min. 20 μL of the substrate solution was added to the wells containing the enzyme and 20 μL of the phosphate buffer solution was added to the remaining wells to keep the total volume constant. The plate was incubated for a further 20 min at 37.5 $^\circ\text{C}$ after which 50 μL of the stop solution (0.1 M Na_2CO_3) was added to all the wells. The absorbance was measured at 25 $^\circ\text{C}$ at a wavelength of 405 nm in the plate reader (Molecular Devices Spectra Max i3X). The final results are reported as the half-maximal inhibitory (IC_{50}) concentration in μM . The results represent the mean of

three independent experiments and are expressed as percentage inhibition calculated as stated below.

$$\text{Inhibitory activity (\%)} = (1 - A/B) \times 100 \quad (1)$$

where A is the absorbance in the presence of the test substance and B is the absorbance of control.

2.6. Alpha-Amylase Assay

The α -amylase inhibition assay was conducted according to the slightly modified standard method [25]. Into a 96-well clear microplate, 50 μ L of the α -amylase buffer solution (maleic acid, sodium chloride, calcium chloride, and sodium azide solution adjusted to pH 6.5 using sodium hydroxide) was added to all the wells. 10 μ L of the α -amylase enzyme solution was added to the odd-numbered wells and 10 μ L of the buffer solution was added to the even-numbered wells. To the designated control wells, 20 μ L of methanol (HPLC grade > 99%) was added and 20 μ L of the sample stock solutions (concentration range between 4 mg/mL to 0.03125 mg/mL) were added in triplicate. The plate was then incubated at 37.5 $^{\circ}$ C for 15 min after which 20 μ L of the starch solution was added to all the wells. The plate was then incubated for a further 20 min at 37.5 $^{\circ}$ C. 50 μ L of the DNS reagent (3,5-dinitrosalicylic acid) was added to stop the reaction and react with the reducing sugars. The plate was then incubated in a covered casing and placed into a water bath at 98.5 $^{\circ}$ C for 20 min. The absorbance was then measured at a wavelength of 540 nm in the plate reader (Molecular Devices Spectra Max i3X). The final results are reported as the half-maximal inhibitory (IC₅₀) concentration in μ M and represent the mean of three independent experiments and are expressed as percentage inhibition calculated by Equation (1).

2.7. Antioxidant Assays

2.7.1. Ferric-Ion Reducing Antioxidant Power (FRAP) Assay

The FRAP assay was evaluated as per previously described methods with slight modification [26]. The FRAP mechanism is based on electron transfer rather than hydrogen atom transfer and is based on the ability of phenols to reduce Fe³⁺ to Fe²⁺ ions by transferring an electron. The reaction is carried out at a pH of 3.6 to maintain iron solubility and to decrease the ionization potential that drives electron transfer. As a result, the redox potential increases resulting in electron transfer being the dominant mechanism [27]. The Fe²⁺ ion in the presence of TPTZ (tripiryridyl triazine) forms a colored complex ($\lambda_{\text{max}} = 593$ nm) which can then be measured using a spectrophotometer to determine the extent of iron reduction by the sample.

The FRAP reagent was prepared using a combination of pre-prepared stock solutions namely the FeCl₃ solution, the TPTZ solution, and the acetate buffer solution. The FeCl₃ solution was prepared by dissolving 0.053 g FeCl₃ into 10 mL H₂O. The TPTZ solution was prepared by dissolving 0.0186 g TPTZ into 6 mL of a 0.1 M HCl solution. The acetate buffer solution was prepared using acetic acid and the conjugate base sodium acetate such that the buffer solution maintained a pH of 3.6. The FRAP reagent was prepared by combining 3 mL of the FeCl₃ solution, 3 mL of the TPTZ solution, 30 mL of the buffer solution, and 6 mL H₂O into a 50 mL test tube. Into a 96-well clear visible range microplate, 10 μ L of the isolated compound stock solutions (**8** and **11** = 1 mg/mL; **9** = 0.0625 mg/mL; **10** = 0.25 mg/mL), as well as the total extract (1 mg/mL) were added into separate microplate wells in triplicate and then mixed with 300 μ L of the FRAP reagent. The microplate was incubated in dark at room temperature for 30 min, after which the plate was read in a Molecular Devices Spectra Max i3X at a wavelength of 593 nm. The standard calibration curve was obtained using L-ascorbic acid (Sigma Aldrich, Johannesburg, South Africa) as a standard. The concentration range was made up between 0 mg/L (blank) and 500 mg/L of L-ascorbic acid for analytical measurement, where each concentration of L-ascorbic acid was measured in triplicate. The results were reported as μ mol ascorbic acid equivalents per mmol (μ mol AAE/mmol) of the dry weight test samples.

2.7.2. Trolox Equivalent Absorbance Capacity (TEAC) Assay

The assay was evaluated as per previously described methods [28]. The TEAC assay measures the ability of antioxidants to scavenge free radicals. In this assay, the stable free radical ABTS⁺ (2,2'-azino-bis(3-ethylbenzothiazoline-6-sulfonic acid)), is a blue-green chromophore ($\lambda_{\max} = 734$ nm) that in the presence of antioxidants decreases its absorption intensity. This occurs by the antioxidants' neutralization of free radicals either by direct reduction (electron transfer) or by hydrogen atom donation. The balance between these two mechanisms is usually determined by the antioxidant structure and the pH of the reaction medium [29].

The working solution was prepared by combining two pre-prepared stock solutions namely, 7 mM ABTS and 140 mM potassium-peroxodisulfate (K₂S₂O₈) (Merck, South Africa). To 5 mL of the ABTS solution, 88 μ L of K₂S₂O₈ solution was added, mixed thoroughly, and then allowed to react in the absence of light for 24 h. Trolox (6-hydroxy-2,5,7,8-tetramethylchroman-2-carboxylic acid), a water-soluble analog of vitamin E, was used as the standard to obtain the standard calibration curve with the concentration range between 0 mg/L and 500 mg/L. Into a 96-well clear microplate, 25 μ L of the isolated compound and total extract stock solutions (1 mg/mL) were added in triplicate wells with 275 μ L of the working solution and allowed to react in the absence of light at room temperature for 30 min. The absorbance was measured at 25 °C at a wavelength of 734 nm in the plate reader. The final results are reported as μ mol Trolox equivalents per mmol (μ mol TE/mmol) of the dry weight test samples.

2.8. Statistical Analysis

All the measurements were repeated three times and the IC₅₀ was calculated using GraphPad Prism 8 version 8.4.3 (Graph pad software, Inc., La Jolla, CA, USA) statistical software. The data presented are means \pm SD obtained from 96 well plate readers for all in vitro experiments.

2.9. Molecular Docking and Molecular Mechanics-Generalized Born Surface Area (MM-GBSA) Calculations

The combined sdf file of compounds 1–11 were imported into Schrodinger Maestro[®] [30] and prepared with the LigPrep wizard [31]. The chiralities, tautomers, and ring conformations of the compounds were corrected and protonated at a physiological pH range of 7 \pm 2. The OPLS3e force field was then used to minimize the protonated compounds.

The X-ray diffraction three-dimensional model (3D) structure of α -Glucosidase (7KRY) and amylase (1B2Y) in the protein data bank was imported into the Schrodinger Maestro[®] as the 3D protein target. The chain A part of the 3D models was isolated and the protein preparation wizard [32–34] was then used to ensure structural correctness, add missing hydrogen atoms, charges, and correct bond orders. The 3D protein target was energy minimized to relieve steric clashes by applying the default constraint of 0.3 Å root-mean-square-deviation (RMSD) and the OPLS3e forcefield.

Before molecular docking, the grid generation panel was used to define a grid box for the binding pocket using the centroid of the co-crystallized ligand in both 3D models. Next, the molecular docking calculation was executed with the ligand docking panel with extra precision (XP) in the Glide module [35]. The binding mode and interaction were visualized with UCSF Chimera [36].

3. Results

3.1. Isolation and Chemical Characterization of Compound Isolated from *H. cymosum* and *H. pandurifolium*

Repeated silica gel and Sephadex column chromatography of the methanolic extract of *H. cymosum* and *H. pandurifolium* yielded seven (1–7) and four (8–11) known flavonoids respectively (Figure 2), the structures of these eleven compounds were confirmed by comparison of spectroscopic data to the literature data.

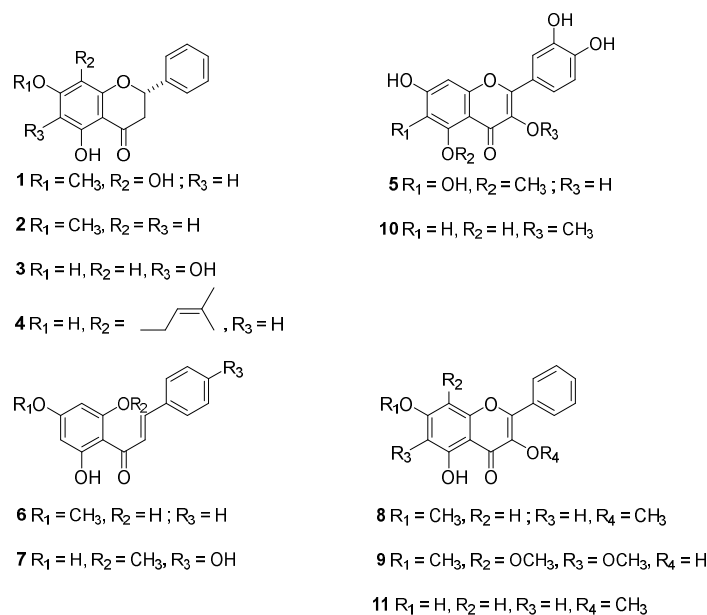


Figure 2. Chemical structures of the isolated compounds from *H. cymosum* (1–7) and *H. pandurifolium* (8–11).

The seven compounds (1–7) isolated from *H. cymosum* (Figure 2) were characterized to be 5,8-dihydroxy-7-methoxy-2-phenyl flavanone (1), pinostrobin (2), dihydrobaicalein (3), glabranin (4), allopaturetin (5), pinostrobin chalcone (6) and helichrysetin (7). Whereas the four compounds (8–11) isolated from *H. pandurifolium* were identified as 5-hydroxy-3,7-dimethoxyflavone (8), 3,5-dihydroxy-6,7,8-trimethoxyflavone (9), 3',4',5,7-tetrahydroxy-3-methoxyflavone (10) and 5,7-dihydroxy-3-methoxyflavone (11). The data of all the isolated compounds were compared to the literature value to corroborate the final chemical structures.

3.2. Alpha-Glucosidase and Alpha-Amylase Activity

The alpha-glucosidase enzyme is situated in the brush border of the small intestine epithelium. It catalyzes the breaking down of the reaction of disaccharides and starch to glucose [37]. Glucosidase inhibitors decrease the rate of carbohydrate digestion and retard carbohydrate absorption from the alimentary tract [38]. In the search for effective hypoglycemic candidates from natural sources, a great deal of research is being carried out to identify phytoconstituents having a hypoglycemic effect with emphasis on the inhibition of alpha-glucosidase and alpha-amylase.

Table 1 presents the IC₅₀ values in μM concentrations for α-glucosidase and α-amylase inhibition by flavonoids (1–11) and in μg/mL for the total methanolic extract of *H. cymosum* and *H. pandurifolium*. Acarbose was used as positive control and was found to have an α-glucosidase inhibition of 945.46 ± 1.0 μM.

An investigation of the inhibitory activities of *H. cymosum* total extract and its natural products showed that 5 demonstrated the highest alpha-glucosidase inhibitory activity with an IC₅₀ value of 12.94 ± 0.2 μM, followed by 7 and 3 with IC₅₀ values of 18.16 ± 1.2 and 44.44 ± 0.2 μM respectively. However, *H. cymosum* total extract and its isolated compounds did not show any measurable inhibition of alpha-amylase enzyme under the experimental conditions used in this study.

Among the compounds isolated from *H. pandurifolium*, the compound 10 showed the highest alpha-glucosidase inhibitory activity with IC₅₀ values of 9.24 ± 0.4 μM whereas compounds 8, 9, and 11 were found to have IC₅₀ values of 103.59 ± 2.4; 86.20 ± 11.16 and 16.00 ± 2.4 μM respectively. Table 1 also presents the IC₅₀ values for α-amylase inhibition by four isolated flavonoids (8–11) and the total methanolic extract of *H. pandurifolium*. Only the flavonoids 3',4',5,7-tetrahydroxy-3-methoxyflavone (compound 10) showed α-amylase

inhibition with an IC₅₀ of 230.66 ± 15.8 µM. Compounds 8 and 11 showed no inhibition up to concentrations of 133 µg/mL.

Table 1. Alpha-glucosidase and alpha-amylase Inhibitory activities (IC₅₀) of total extracts and phytochemical constituents of *H. cymosum* and *H. pandurifolium*.

Sample	α-Glucosidase Inhibition IC ₅₀ (µM)	α-Amylase Inhibition IC ₅₀ (µM)
1	NA	NA
2	204.23 ± 1.1	NA
3	44.44 ± 0.2	NA
4	NA	NA
5	12.94 ± 0.2	NA
6	206.45 ± 0.7	NA
7	18.16 ± 1.2	NA
8	103.59 ± 2.4	NA
9	86.20 ± 11.6	NA
10	9.24 ± 0.4	230.66 ± 15.8
11	16.00 ± 2.4	NA
<i>H. cymosum</i> (TE) *	35.8 ± 0.3	NA
<i>H. pandurifolium</i> (TE) *	69.28 ± 14.3	NA
Acarbose	945.46 ± 1.0	15.80 ± 0.6

* For total extract of *H. cymosum* and *H. pandurifolium* IC₅₀ is expressed as µg/mL. NA = showed no measurable activity using the specified method of analysis. The results are expressed as mean ± SEM for n = 3.

3.3. Antioxidant Activity

Oxidative stress is well known as one of the principal causes of diabetic complications due to the accumulation of free radicals, which cause mitochondrial superoxide overproduction, β-cell dysfunction, and diabetes vascular damage [39]. The in vitro antioxidant activity of the isolated compounds from *H. cymosum* and *H. pandurifolium* was investigated by evaluating their ferric ion reducing antioxidant power (FRAP) and Trolox Equivalent Absorbance Capacity (TEAC) activities. TEAC is an assay based on a hydrogen atom transfer (HAT) mechanism [40], while FRAP is based on a single electron transfer (SET) mechanism [41].

The results of the in vitro antioxidant activity study demonstrated that compounds 5 and 7 showed strong activity on FRAP (334.37 ± 1.7; 279.93 ± 0.8) µmol AAE/mmol, followed by compound 1 which showed a moderate activity (185.72 ± 1.1) µmol AAE/mmol as shown in Table 2.

Table 2. Antioxidant activities of *H. cymosum* constituents and *H. pandurifolium*.

Sample	FRAP (µmol AAE/mmol)	TEAC (µmol TE/mmol)
1	185.72 ± 1.1	NA
2	53.35 ± 0.7	NA
3	8.44 ± 0.24	NA
4	11.75 ± 0.9	NA
5	334.37 ± 1.7	NA
6	25.33 ± 0.6	NA
7	279.93 ± 0.8	NA
8	NA	73.62 ± 2.9
9	93.93 ± 7.1	275.39 ± 8.6
10	374.34 ± 69.7	301.37 ± 1.5
11	5.00 ± 2.8	138.33 ± 3.7
<i>H. cymosum</i> (TE) *	NA	NA
<i>H. pandurifolium</i> (TE) *	248.2 ± 0.1	722.4 ± 16.6
Acarbose	4858.29 ± 4.9	2677.00 ± 19.8

* For total extract of *H. cymosum* and *H. pandurifolium* IC₅₀ is expressed as µg/mL. NA = showed no measurable activity using the specified method of analysis. The results are expressed as mean ± SEM for n = 3.

Table 2 also summarises the antioxidant capacities measured for the total extract of *H. pandurifolium* and its four isolated flavonoids. Compound 10 was found to be the phytochemical with the greatest antioxidant capacity of the four compounds isolated from *H. pandurifolium*.

3.4. Molecular Docking

The molecular docking of compounds 1 to 11 and acarbose as a reference on the active sites of the 3D model of alpha-glucosidase (neutral alpha-glucosidase ab chain A) and alpha-amylase showed free binding energy ranging from -5.7 kcal/mol to -13.07 kcal/mol for alpha-glucosidase and -4.0 kcal/mol to 12.06 kcal/mol for alpha-amylase (Figure 3).

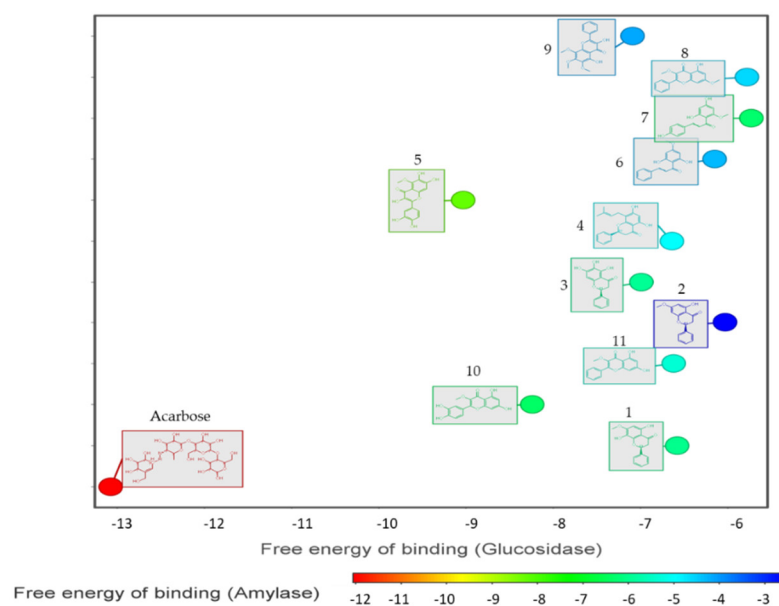


Figure 3. The free binding energy of compounds 1–11 and acarbose to the active sites of alpha-glucosidase and amylase.

It was observed that some of the active compounds from the in vitro alpha-glucosidase assay (compounds 5, 10, and 11) have a stronger binding affinity (free energy of binding) for the enzymes than the other compounds. A closer look at these compounds and their interaction with the active site of the alpha-glucosidase 3D model revealed a hydrogen bond (at a minimum distance of 2.5 Å and 20° angles) with amino acid residues at the active site (Figure 4).

Alpha glucosidases cleave dietary starch and oligosaccharides into glucose. A potential inhibitor of alpha-glucosidase should block the substrate-binding active site of the enzyme, thereby preventing the oligosaccharides from accessing the active site. Within the active site are two highly conserved and important residues that are pivotal for the binding of substrates to the enzyme: Asp564 acts as the catalytic nucleophile and Asp640 act as the acid/base catalyst [42]. Therefore, interactions with the catalytic nucleophile Asp564 and acid/base catalyst Asp640 amino acid residues might be a predictor of alpha-glucosidase inhibition. Compounds 5 and 10 showed two hydrogen bond interactions with catalytic nucleophile Asp564 and one interaction with acid/base catalyst Asp640. Compound 11 showed two interactions with catalytic nucleophile Asp564 but no interaction with acid/base catalyst Asp640. This may account for the observed inhibitory activities. Compound 7 showed no interaction with either of the residues, the reported inhibitory activity from the in vitro assay might be due to its van der Waals interactions with Asp640.

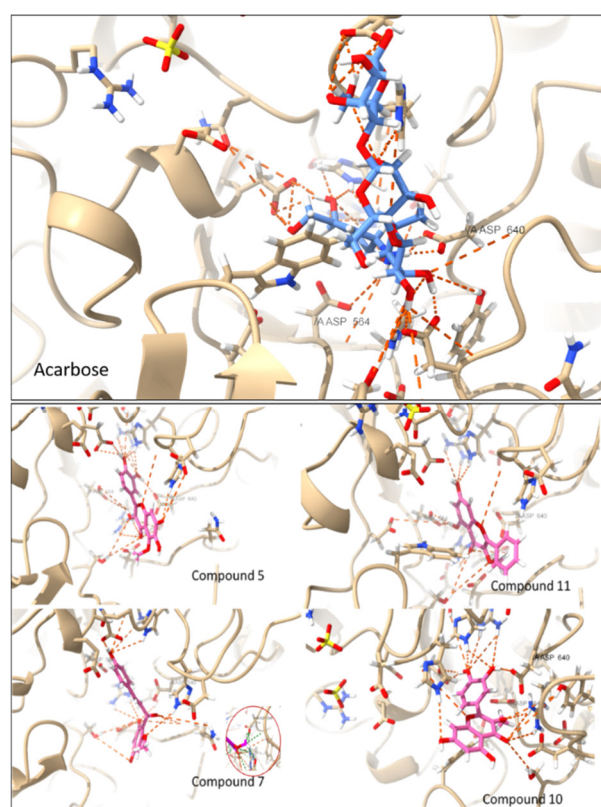


Figure 4. Active site amino acid residue interaction analysis of the acarbose (top panel) and the top docked poses of compounds 5, 7, 10, 11 with alpha-glucosidase. Compound 5 showed 20 hydrogen bond interactions with active site residues (including catalytic nucleophile Asp564 and acid/base catalyst Asp640 amino acid residues) while compounds 10 and 11 showed 16 and 11 hydrogen bond interactions respectively with active site residues. Compound 7 showed 14 hydrogen bond interactions (no hydrogen bond interactions with the catalytic nucleophile Asp564 and acid/base catalyst Asp640 amino acid residues but three Van der Waals interactions with Asp640).

4. Discussion

The structures of the isolated compounds were confirmed by comparing their spectroscopic data to the reported data in the literature. Compound 1 has been reported to be isolated from *Echiochilon fruticosum* [43] and it showed antioxidant, anti-inflammatory, and hepatoprotective properties [44]. Compound 2, isolated from *H. gymnocomum* and *Echiochilon fruticosum* [20,43,45], showed antibacterial, anti-inflammatory, antitumor, antidiarrhea, anti-HIV, antioxidant, and antipyretic activities [46]. Isolation of compound 3 was reported to be from *Scutellaria baicalensis* [47] and it showed a wide range of biological activities including anticancer [48]. Compound 4 was isolated previously from *H. cymosum* and *H. teretifolium* [19,21] and it showed antibacterial and antioxidant activities [49]. Compound 5 was isolated from *Xanthium strumarium* [50], which also belongs to the same family Asteraceae and it possesses antibacterial and antifungal activities [51]. Compound 6 was isolated from *Helichrysum trilineatum* and extracts of *Piper clausenianum* and demonstrated antidiabetic and antibacterial activities [52,53]. Compound 7 was isolated from *Helichrysum odoratissimum* and was reported to possess a wide range of pharmaceutical applications including antiproliferative, anticancer, antiplatelet, and antioxidant [54].

Compound 8 was previously isolated from *Kaempferia parviflora* [55]. Compound 9 was reported from *H. decumbens* and *H. graveolens* [56], compound 10 was isolated from *Halimodendron halodendron* [57] whereas, the compound 11 was isolated from *Alipinia officinarum* and showed pancreatic lipase inhibitory activity [58].

The alpha-glucosidase inhibitory activity of the isolated compounds (1–11) from both *H. cymosum* and *H. pandurifolium* revealed the compounds 10, 5, 11, and 7 to be the most

active with compound **10** exhibiting the highest activity followed by compounds **5**, **11**, and **7**. Among the compounds isolated from *H. cymosum*, **5** and **7** showed the highest alpha-glucosidase inhibition whereas compounds **10** and **11** showed the highest inhibition among compounds isolated from *H. pandurifolium*. None of the isolated compounds showed any assessable inhibitory effect on alpha-amylase under the experimental conditions used except compound **10** which showed a poor alpha-amylase inhibitory activity.

Compound **7**, Helichrysetin, has not been reported to possess hypoglycemic activity. However, phloretin, which belongs to the same class of compounds as **7**, has been reported to exhibit strong reversible alpha-glucosidase inhibitory activity in a mixed-type manner with an IC₅₀ value of 31.26 µg/L [59]. Its glucoside (phlorizin) inhibits the sodium-dependent glucose transporters (SGLT1 and SGLT2) resulting in the reduction of the absorption and reabsorption of glucose from the small intestine and kidneys by SGLT1 and SGLT2 respectively [60]. Synthetic derivatives of phlorizin are clinically used in the treatment of diabetes [61]. Compound **7** has also been reported to exert a hypoglycemic effect in streptozotocin-induced diabetic rats and reduces insulin resistance [62]. On the other hand, pinostrobin chalcone (**6**) has been reported to be responsible for the reduction of blood glucose levels in rats with streptozotocin-induced diabetes [53]. Unfortunately, in this study, this compound showed moderate activity when tested for the alpha-glucosidase enzyme. Remarkably, the SAR studies demonstrated that the more polar compounds among the tested (**1–7**) exhibited the highest activities.

The enzymatic inhibition results of compounds (**8–11**) isolated *H. pandurifolium* were in accordance with the SAR studies as previously described by Proença et al. for both α-glucosidase and α-amylase [11,12]. The greater inhibitory effect of compound **10** on alpha-glucosidase and alpha-amylase enzymes can be attributed to the catechol group on ring-B, hydroxy-functional groups at 5-, 7-, or 8-position of ring-A, and the C2=C3 double bond in ring-C, all of which are crucial for significant flavonoid α-glucosidase and α-amylase activity. In literature, the flavonoids have been reported to possess significant antidiabetic activity due to the hydroxyl group allocated at C-3 on the A-ring and additional hydroxyl groups attached to the C-ring, which play an important role in the inhibition process of the alpha-glucosidase enzyme as well as hypoglycemia, insulin activation, glucose uptake activation [63]. Additionally, flavonoids are commonly used in antidiabetic diets and many of them include catechins, fisetin, kaempferol, luteolin, naringenin, quercetin, rutin, morin, silymarin, chrysin, baicalein, icariin, isoliquiritigenin, diosmin, isoangustone A and genistein were reported to be active for their antidiabetic properties [64].

It is proposed that to further establish these compounds as potential hypoglycemic agents, their inhibitory effect on other glucose regulating enzymes and the enzymes for lipid digestion and absorption should be investigated. This would further pave the way for in vivo studies of the promising hypoglycemic candidates in these investigations. It is envisaged that the results of in vivo studies would give us an indication of the possible doses appropriate for use in humans.

In antioxidant study experiments, compounds **5** and **7** from *H. cymosum* and compound **10** from *H. pandurifolium* displayed the highest activities. Compounds **5** and **7** have already been reported to be good candidates to serve as safe antioxidants [65]. The essential oil of *H. cymosum* has been reported to possess radical scavenging activity with an SC₅₀ (concentration that causes 50% free radical scavenging) value of 6.3 mg/mL [66]. Phenolic compounds have been reported to be responsible for the antioxidant activity of numerous plant species by stabilization of free radicals by donating electrons or by metal ion complexation among other mechanisms. Nevertheless, other aspects can be considered, for example, the presence of vicinal hydroxyl groups is essential in a pronounced antioxidant activity [67]. Flavonoids represent a very large class of plant secondary metabolites found in a wide range of fruits, vegetables, and herbs that can play a prominent role as natural antioxidants, due to the presence of hydroxyl groups and aromatic rings in their chemical structures [68]. In general, the presence of a pair of hydroxyls at *ortho* position to each other (catechol configuration) on the B-ring is the most important active group, for the

hydrogen atom transfer/single electron transfer to the hydroxyl/peroxyl radicals, thereby stabilizing them and giving rise to a relatively stable flavonoid radical [69]. Our results are therefore an indication that **7** and **2** have great capacities for hydrogen atom(s) transfer from B-hydroxyl groups to stabilize free radicals.

The highest antioxidant activity of compound **10** is in accordance with the theory that more hydroxyl functional groups on the flavan backbone structure lead to greater antioxidant activity, as described in previous studies [70,71]. This also confirms the significance of the 3'- and 4'-hydroxy groups (catechol) on the B-ring. Compound **8** on the other hand, having only one free OH at position 5, showed no significant activity in the FRAP antioxidant assay and relatively low activity in the TEAC antioxidant assay when compared to the other compounds. Compound **11** showed similar, relatively low antioxidant activity in the FRAP assay likely due to the methylated hydroxyl functional group at position 3. The significance of the free hydroxy on the C-3 is evident from the FRAP assay results, where compound **9**, the only compound with a free 3-OH, yields significantly greater antioxidant activity when compared to the others (excluding **10**), even though the positions C-6, C-7, and C-8 are all methoxylated. The total methanolic extract of *H. pandurifolium*, when compared to other methanolic extracts of *Helichrysum*, showed FRAP antioxidant activity of 43.7 ± 0.1 mg AAE/g, significantly lower than those of the various other *Helichrysum* species summarised by Albayrak, et al. [72].

Overall, the molecular docking gave insight into the observed results from the in vitro inhibitory alpha-glucosidase assay. The only major departure was observed for acarbose (the reference drug which is a known inhibitor of alpha-glucosidase). The molecular docking aligned with the reported use of acarbose as a potent inhibitor of alpha-glucosidase by the predicted high negative free binding energy (over -13 kcal/mol). The departure observed for in vitro inhibitory activity might be due to non-optimal assay conditions for acarbose (which is a maltotetrose analog, possessing a free end that may act as a reducing agent). An excessive amount of acarbose in the assay medium might react with 3, 5, di-nitro salicylic acid (DNS) (the chromophore for this colorimetric assay) thereby causing a substantial ~ 5 -fold effect on acarbose IC_{50} values when working just outside optimal concentration range [73].

5. Conclusions

The phytochemical analysis of the methanolic extracts of *H. cymosum* and *H. pandurifolium* yielded eleven known flavonoids. Their structure was elucidated by NMR spectroscopy and the spectroscopy data of the isolated compounds was compared to the literature data. The in vitro bio-evaluation of the extracts and their phytoconstituents revealed these plants to be a potential source of flavonoids with strong alpha-glucosidase inhibitory activities as well as significant antioxidant activity. These plants might become prominent natural therapeutic agents for the inhibition of alpha-glucosidase and oxidative stress, which play an important role in diabetic complications.

The present work is the first scientific report on alpha-glucosidase inhibitory activities and antioxidant capacities of *H. cymosum* constituents. This work is also the first scientific report on the phytochemical analysis of *H. pandurifolium* and the first inhibitory activity study of its total methanolic extract and its flavonoids on α -glucosidase and α -amylase.

Author Contributions: Designing and performing of experiments and manuscript drafting, B.M.I.S.J., J.J.M. and N.G.E.R.E.; project supervision, and manuscript drafting, R.S.; biological activity experiments, data curation, and manuscript drafting, J.A.B. and J.L.M.; Computational simulations, analysis, and write-up, S.A.E.; characterization of compounds, conceptualization, project supervision, and manuscript review, A.A.H.; and project supervision and manuscript review, D.B.; validation, writing—review and editing, C.N.C. All authors have read and agreed to the published version of the manuscript.

Funding: This research was funded by The National Research Foundation (NRF) of South Africa, grant number NRF CPRR160506164193.

Institutional Review Board Statement: Not applicable.

Informed Consent Statement: Not applicable.

Data Availability Statement: Not applicable.

Acknowledgments: NMR facilities at UWC and CPUT.

Conflicts of Interest: The authors declare no conflict of interest.

References

1. Astrup, A. Healthy lifestyles in Europe: Prevention of obesity and type II diabetes by diet and physical activity. *Public Health Nutr.* **2001**, *4*, 499–515. [[CrossRef](#)] [[PubMed](#)]
2. Duckworth, W.C. Hyperglycemia and cardiovascular disease. *Curr. Atheroscler. Rep.* **2001**, *3*, 383–391. [[CrossRef](#)] [[PubMed](#)]
3. Cho, N.; Shaw, J.E.; Karuranga, S.; Huang, Y.; da Rocha Fernandes, J.D.; Ohlrogge, A.W.; Malanda, B. IDF Diabetes Atlas: Global estimates of diabetes prevalence for 2017 and projections for 2045. *Diabetes Res. Clin. Pract.* **2018**, *138*, 271–281. [[CrossRef](#)] [[PubMed](#)]
4. Gao, K.; Zheng, C.; Wang, T.; Zhao, H.; Wang, J.; Wang, Z.; Zhai, X.; Jia, Z.; Chen, J.; Zhou, Y.; et al. 1-Deoxynojirimycin: Occurrence, extraction, chemistry, oral pharmacokinetics, biological activities and in silico target fishing. *Molecules* **2016**, *21*, 1600. [[CrossRef](#)]
5. Mamun-or-Rashid, A.N.; Hossain, M.S.; Hassan, N.; Dash, B.K.; Sapon, M.A.; Sen, M.K. A review on medicinal plants with antidiabetic activity. *J. Pharmacogn. Phytochem.* **2014**, *3*, 149–159.
6. Ullah, A.; Khan, A.; Khan, I. Diabetes mellitus and oxidative stress—A concise review. *Saudi Pharm. J.* **2016**, *24*, 547–553. [[CrossRef](#)]
7. Chaudhury, A.; Duvoor, C.; Reddy Dendi, V.S.; Kraleti, S.; Chada, A.; Ravilla, R.; Marco, A.; Shekhawat, N.S.; Montales, M.T.; Kuriakose, K.; et al. Clinical review of antidiabetic drugs: Implications for type 2 diabetes mellitus management. *Front. Endocrinol.* **2017**, *8*, 6. [[CrossRef](#)]
8. Jung, M.; Park, M.; Lee, H.C.; Kang, Y.H.; Kang, E.S.; Kim, S.K. Antidiabetic agents from medicinal plants. *Curr. Med. Chem.* **2006**, *13*, 1203–1218. [[CrossRef](#)]
9. Tadera, K.; Minami, Y.; Takamatsu, K.; Matsuoka, T. Inhibition of α -glucosidase and α -amylase by flavonoids. *J. Nutr. Sci. Vitaminol.* **2006**, *52*, 149–153. [[CrossRef](#)]
10. Ahmed, D.; Kumar, V.; Sharma, M.; Verma, A. Target guided isolation, in-vitro antidiabetic, antioxidant activity and molecular docking studies of some flavonoids from *Albizzia lebeck* Benth. bark. *BMC Complement. Altern. Med.* **2014**, *14*, 155. [[CrossRef](#)]
11. Proença, C.; Freitas, M.; Ribeiro, D.; Oliveira, E.F.; Sousa, J.L.; Tomé, S.M.; Ramos, M.J.; Silva, A.M.; Fernandes, P.A.; Fernandes, E. α -Glucosidase inhibition by flavonoids: An in vitro and in silico structure–activity relationship study. *J. Enzyme Inhib. Med. Chem.* **2017**, *32*, 1216–1228. [[CrossRef](#)] [[PubMed](#)]
12. Proença, C.; Freitas, M.; Ribeiro, D.; Tomé, S.M.; Oliveira, E.F.; Viegas, M.F.; Araújo, A.N.; Ramos, M.J.; Silva, A.M.; Fernandes, P.A.; et al. Evaluation of a flavonoids library for inhibition of pancreatic α -amylase towards a structure–activity relationship. *J. Enzym. Inhib. Med. Chem.* **2019**, *34*, 577–588. [[CrossRef](#)] [[PubMed](#)]
13. Abbas, G.; Al Harrasi, A.; Hussain, H.; Hamaed, A.; Supuran, C.T. The management of diabetes mellitus—imperative role of natural products against dipeptidyl peptidase-4, α -glucosidase and sodium-dependent glucose co-transporter 2 (SGLT2). *Bioorg. Chem.* **2019**, *86*, 305–315. [[CrossRef](#)] [[PubMed](#)]
14. Lourens, A.C.; Viljoen, A.M.; Van Heerden, F.R. South African *Helichrysum* species: A review of the traditional uses, biological activity and phytochemistry. *J. Ethnopharmacol.* **2008**, *119*, 630–652. [[CrossRef](#)]
15. Mhlongo, L.S.; Van Wyk, B.E. Zulu medicinal ethnobotany: New records from the Amandawe area of KwaZulu-Natal, South Africa. *S. Afr. J. Bot.* **2019**, *122*, 266–290. [[CrossRef](#)]
16. Maroyi, A. Medicinal uses, biological and phytochemical properties of *Helichrysum foetidum* (L.) Moench (Asteraceae). *Asian J. Pharm. Clin. Res.* **2019**, *12*, 13–18. [[CrossRef](#)]
17. Heyman, H.M. Identification of Anti-HIV Compounds in *Helichrysum* Species (Asteraceae) by Means of NMR-Based Metabolomic Guided Fractionation. Doctoral Dissertation, University of Pretoria, Tswane, South Africa, 2013.
18. Maroyi, A.L. *Helichrysum cymosum* (L.) D. Don (Asteraceae): Medicinal uses, chemistry, and biological activities. *Asian J. Pharm. Clin. Res.* **2019**, *12*, 19–26. [[CrossRef](#)]
19. Jakupovic, J.; Zdero, C.; Grenz, M.; Tschritzis, F.; Lehmann, L.; Hashemi-Nejad, S.M.; Bohlmann, F. Twenty-one acylphloroglucinol derivatives and further constituents from South African *Helichrysum* species. *Phytochemistry* **1989**, *28*, 1119–1131. [[CrossRef](#)]
20. Van Vuuren, S.F.; Viljoen, A.M.; Van Zyl, R.L.; Van Heerden, F.R.; Başer, K.H. The antimicrobial, antimalarial and toxicity profiles of helihumulone, leaf essential oil and extracts of *Helichrysum cymosum* (L.) D. Don subsp. *cymosum*. *S. Afr. J. Bot.* **2006**, *72*, 287–290. [[CrossRef](#)]
21. Popoola, O.K.; Marnewick, J.L.; Rautenbach, F.; Ameer, F.; Iwuoha, E.I.; Hussein, A.A. Inhibition of oxidative stress and skin aging-related enzymes by prenylated chalcones and other flavonoids from *Helichrysum teretifolium*. *Molecules* **2015**, *20*, 7143–7155. [[CrossRef](#)]

22. Lourens, A.C.; Van Vuuren, S.F.; Viljoen, A.M.; Davids, H.; Van Heerden, F.R. Antimicrobial activity and in vitro cytotoxicity of selected South African *Helichrysum* species. *S. Afr. J. Bot.* **2011**, *77*, 229–235. [[CrossRef](#)]
23. Akinyede, K.A.; Cupido, C.N.; Hughes, G.D.; Oguntibeju, O.O.; Ekpo, O.E. Medicinal Properties and In Vitro Biological Activities of Selected *Helichrysum* Species from South Africa: A Review. *Plants* **2021**, *10*, 1566. [[CrossRef](#)] [[PubMed](#)]
24. Etsassala, N.G.; Badmus, J.A.; Marnewick, J.L.; Egieyeh, S.; Iwuoha, E.; Nchu, F.; Hussein, A.A. Alpha-Glucosidase and Alpha-Amylase Inhibitory Activities, Molecular Docking, and Antioxidant Capacities of *Plectranthus ecklonii* Constituents. *Antioxidants* **2022**, *11*, 378. [[CrossRef](#)] [[PubMed](#)]
25. Etsassala, N.G.; Badmus, J.A.; Marnewick, J.L.; Iwuoha, E.I.; Nchu, F.; Hussein, A.A. Alpha-glucosidase and alpha-amylase inhibitory activities, molecular docking, and antioxidant capacities of *Salvia aurita* constituents. *Antioxidants* **2020**, *9*, 1149. [[CrossRef](#)]
26. Benzie, I.F.; Strain, J.J. The ferric reducing ability of plasma (FRAP) as a measure of “antioxidant power”: The FRAP assay. *Anal. Biochem.* **1996**, *239*, 70–76. [[CrossRef](#)]
27. Cerretani, L.; Bendini, A. Rapid assays to evaluate the antioxidant capacity of phenols in virgin olive oil. In *Olives and Olive Oil in Health and Disease Prevention*; Academic Press: Cambridge, MA, USA, 2010; pp. 625–635. [[CrossRef](#)]
28. Nicoletta, P. Screening of dietary carotenoids and carotenoid-rich fruit extracts for antioxidant activities applying 2,2'-azinobis (3-ethylbenzothiazoline-6-sulfonic acid) radical cation decolorization assay. *Method Enzymol.* **1999**, *299*, 379–389. [[CrossRef](#)]
29. Zhong, Y.; Shahidi, F. Methods for the assessment of antioxidant activity in foods. In *Handbook of Antioxidants for Food Preservation*; Woodhead Publishing: Sawston, UK, 2015; pp. 287–333. [[CrossRef](#)]
30. *Schrödinger Release 2021-4: Maestro*; Schrödinger, LLC: New York, NY, USA, 2021.
31. *Schrödinger Release 2021-4: LigPrep*; Schrödinger, LLC: New York, NY, USA, 2021.
32. *Schrödinger Release 2021-4: Protein Preparation Wizard*; Epik, Schrödinger, LLC: New York, NY, USA, 2021.
33. *Schrödinger Release 2021-4: Impact*; Schrödinger, LLC: New York, NY, USA, 2021.
34. *Schrödinger Release 2021-4: Prime*; Schrödinger, LLC: New York, NY, USA, 2021.
35. *Schrödinger Release 2021-4: Glide*; Schrödinger, LLC: New York, NY, USA, 2021.
36. Pettersen, E.F.; Goddard, T.D.; Huang, C.C.; Couch, G.S.; Greenblatt, D.M.; Meng, E.C.; Ferrin, T.E. UCSF Chimera—A visualization system for exploratory research and analysis. *J. Comput. Chem.* **2004**, *25*, 1605–1612. [[CrossRef](#)]
37. Gericke, B.; Schecker, N.; Amiri, M.; Naim, H.Y. Structure-function analysis of human sucrase-isomaltase identifies key residues required for catalytic activity. *J. Biol. Chem.* **2017**, *292*, 11070–11078. [[CrossRef](#)]
38. Bajpai, V.K.; Kang, S.C. Tyrosinase and α -glucosidase inhibitory effects of an abietane type diterpenoid taxodone from *Metasequoia glyptostroboides*. *Natl. Acad. Sci. Lett.* **2015**, *38*, 399–402. [[CrossRef](#)]
39. Giacco, F.; Brownlee, M. Oxidative stress and diabetic complications. *Circ. Res.* **2010**, *107*, 1058–1070. [[CrossRef](#)]
40. Apak, R.; Özyürek, M.; Güçlü, K.; Çapanoğlu, E. Antioxidant activity/capacity measurement. 2. Hydrogen atom transfer (HAT)-based, mixed-mode (electron transfer (ET)/HAT), and lipid peroxidation assays. *J. Agric. Food. Chem.* **2016**, *64*, 1028–1045. [[CrossRef](#)] [[PubMed](#)]
41. Pérez-Fons, L.; Garzon, M.T.; Micol, V. Relationship between the antioxidant capacity and effect of rosemary (*Rosmarinus officinalis* L.) polyphenols on membrane phospholipid order. *J. Agric. Food. Chem.* **2010**, *58*, 161–171. [[CrossRef](#)] [[PubMed](#)]
42. Karade, S.S.; Hill, M.L.; Kiappes, J.L.; Manne, R.; Aakula, B.; Zitzmann, N.; Warfield, K.L.; Treston, A.M.; Mariuzza, R.A. N-Substituted Valiolamine Derivatives as Potent Inhibitors of Endoplasmic Reticulum α -Glucosidases I and II with Antiviral Activity. *J. Med. Chem.* **2021**, *64*, 18010–18024. [[CrossRef](#)]
43. Hammami, S.; Jannet, H.B.; Bergaoui, A.; Ciavatta, L.; Cimino, G.; Mighri, Z. Isolation and structure elucidation of a flavanone, a flavanone glycoside and vomifoliol from *Echiochilon fruticosum* growing in Tunisia. *Molecules* **2004**, *9*, 602–608. [[CrossRef](#)] [[PubMed](#)]
44. Andrade-Carrera, B.; Clares, B.; Noé, V.; Mallandrich, M.; Calpena, A.C.; García, M.L.; Garduño-Ramírez, M.L. Cytotoxic evaluation of (2S)-5,7-dihydroxy-6-prenylflavanone derivatives loaded PLGA nanoparticles against MiaPaCa-2 cells. *Molecules* **2017**, *22*, 1553. [[CrossRef](#)] [[PubMed](#)]
45. Drewes, S.E.; van Vuuren, S.F. Antimicrobial acylphloroglucinols and dibenzylxy flavonoids from flowers of *Helichrysum gymnocomum*. *Phytochemistry* **2008**, *69*, 1745–1749. [[CrossRef](#)] [[PubMed](#)]
46. Marliyana, S.D.; Mujahidin, D.; Syah, Y.M. Pinostrobin Derivatives from Prenylation Reaction and their Antibacterial Activity against Clinical Bacteria. *IOP Conf. Ser. Mater. Sci. Eng.* **2018**, *349*, 012057. [[CrossRef](#)]
47. Woo, S.U.; Jang, H.R.; Chin, Y.W.; Yim, H. 7-O-Methylwogonin from *Scutellaria baicalensis* disturbs mitotic progression by inhibiting Plk1 activity in Hep3B cells. *Planta Med.* **2019**, *85*, 217–224. [[CrossRef](#)]
48. Chae, H.S.; Xu, R.; Won, J.Y.; Chin, Y.W.; Yim, H. Molecular targets of genistein and its related flavonoids to exert anticancer effects. *Int. J. Mol. Sci.* **2019**, *20*, 2420. [[CrossRef](#)]
49. Gupta, A.; Maheshwari, D.K.; Khandelwal, G. Antibacterial activity of *Glycyrrhiza glabra* roots against certain gram-positive and gram-negative bacterial strains. *J. Appl. Nat. Sci.* **2013**, *5*, 459–464. [[CrossRef](#)]
50. Fan, W.; Fan, L.; Peng, C.; Zhang, Q.; Wang, L.; Li, L.; Wang, J.; Zhang, D.; Peng, W.; Wu, C. Traditional uses, botany, phytochemistry, pharmacology, pharmacokinetics and toxicology of *Xanthium strumarium* L.: A review. *Molecules* **2019**, *24*, 359. [[CrossRef](#)] [[PubMed](#)]

51. Faizi, S.; Siddiqi, H.; Bano, S.; Naz, A.; Lubna; Mazhar, K.; Nasim, S.; Riaz, T.; Kamal, S.; Ahmad, A.; et al. Antibacterial and antifungal activities of different parts of *Tagetes patula*: Preparation of patuletin derivatives. *Pharm. Biol.* **2008**, *46*, 309–320. [[CrossRef](#)]
52. Bremner, P.D.; Meyer, J.J. Pinocembrin chalcone: An antibacterial compound from *Helichrysum trilineatum*. *Planta Med.* **1998**, *64*, 777. [[CrossRef](#)] [[PubMed](#)]
53. Marques, A.M.; Pereira, S.L.; Paiva, R.A.; Cavalcante, C.V.; Sudo, S.Z.; Tinoco, L.W.; Moreira, D.L.; Guimaraes, E.F.; Sudo, R.T.; Kaplan, M.A.; et al. Hypoglycemic effect of the methanol flower extract of piper clausenianum and the major constituent 2',6'-dihydroxy-4'-methoxychalcone in streptozotocin diabetic rats. *Indian J. Pharm. Sci.* **2015**, *77*, 237–243. [[CrossRef](#)]
54. Ho, Y.F.; Karsani, S.A.; Yong, W.K.; Abd Malek, S.N. Induction of apoptosis and cell cycle blockade by helichrysetin in a549 human lung adenocarcinoma cells. *Evid. Based Complement. Altern. Med.* **2013**, *2013*, 857257. [[CrossRef](#)]
55. Sutthanut, K.; Sripanidkulchai, B.; Yenjai, C.; Jay, M. Simultaneous identification and quantitation of 11 flavonoid constituents in *Kaempferia parviflora* by gas chromatography. *J. Chromatogr. A* **2007**, *1143*, 227–233. [[CrossRef](#)]
56. Tomás-Lorente, F.; Iniesta-Sanmartín, E.; Tomás-Barberán, F.A.; Trowitzsch-Kienast, W.; Wray, V. Antifungal phloroglucinol derivatives and lipophilic flavonoids from *Helichrysum decumbens*. *Phytochemistry* **1989**, *28*, 1613–1615. [[CrossRef](#)]
57. Wang, J.; Gao, H.; Zhao, J.; Wang, Q.; Zhou, L.; Han, J.; Yu, Z.; Yang, F. Preparative separation of phenolic compounds from *Halimodendron halodendron* by high-speed counter-current chromatography. *Molecules* **2010**, *15*, 5998–6007. [[CrossRef](#)]
58. Shin, J.E.; Han, M.J.; Kim, D.H. 3-Methylethergalangin isolated from *Alpinia officinarum* inhibits pancreatic lipase. *Biol. Pharm. Bull.* **2003**, *26*, 854–857. [[CrossRef](#)]
59. Han, L.; Fang, C.; Zhu, R.; Peng, Q.; Li, D.; Wang, M. Inhibitory effect of phloretin on α -glucosidase: Kinetics, interaction mechanism and molecular docking. *Int. J. Biol. Macromol.* **2017**, *95*, 520–527. [[CrossRef](#)]
60. Liu, J.; Lee, T.; DeFronzo, R.A. Why do SGLT2 inhibitors inhibit only 30–50% of renal glucose reabsorption in humans? *Diabetes* **2012**, *61*, 2199–2204. [[CrossRef](#)] [[PubMed](#)]
61. Liu, J.J.; Lee, T. SGLT2 inhibitors for type 2 diabetes. In *Annual Reports in Medicinal Chemistry*; Academic Press: Cambridge, MA, USA, 2011; Volume 46, pp. 103–115. [[CrossRef](#)]
62. Shen, X.; Zhou, N.; Mi, L.; Hu, Z.; Wang, L.; Liu, X.; Zhang, S. Phloretin exerts hypoglycemic effect in streptozotocin-induced diabetic rats and improves insulin resistance in vitro. *Drug Des. Dev. Ther.* **2017**, *11*, 313–324. [[CrossRef](#)] [[PubMed](#)]
63. Wang, H.; Du, Y.J.; Song, H.C. α -Glucosidase and α -amylase inhibitory activities of guava leaves. *Food Chem.* **2010**, *123*, 6–13. [[CrossRef](#)]
64. Den Hartogh, D.J.; Tsiani, E. Antidiabetic properties of naringenin: A citrus fruit polyphenol. *Biomolecules* **2019**, *9*, 99. [[CrossRef](#)]
65. Shindo, K.; Kato, M.; Kinoshita, A.; Kobayashi, A.; Koike, Y. Analysis of antioxidant activities contained in the *Boesenbergia pandurata* Schult. rhizome. *Biosci. Biotechnol. Biochem.* **2006**, *70*, 2281–2284. [[CrossRef](#)]
66. Francois, T.; Lambert, S.M.; Michel, J.D.P.; Gaby, N.M.E.; Fabrice, F.B.; Zaché, N.; Henri, A.Z.P.; Chantal, M. Composition, radical scavenging and antifungal activities of essential oils from 3 *Helichrysum* species growing in Cameroon against *Penicillium oxalicum* a yam rot fungi. *Afr. J. Agric. Res.* **2010**, *5*, 121–127. [[CrossRef](#)]
67. Souza de Oliveira, F.F.; Coleho, P.N.; Gomes, G.J.; de Amorim, M.L.; Santos, P.S.; Mendonça, C.V.; Gonçalves, R.R.; Lins, M.G.; Pio, W.T.; Fuzer, C.F. Antioxidant Activity and Phytochemical Screening of Extracts of *Erythroxylum suberosum* A. St.-Hil (Erythroxylaceae). *Res. J. Phytochem.* **2015**, *9*, 68–78. [[CrossRef](#)]
68. Panche, A.N.; Diwan, A.D.; Chandra, S.R. Flavonoids: An overview. *J. Nutr. Sci.* **2016**, *5*, e47. [[CrossRef](#)]
69. Wolfe, K.L.; Kang, X.; He, X.; Dong, M.; Zhang, Q.; Liu, R.H. Cellular antioxidant activity of common fruits. *J. Agric. Food Chem.* **2008**, *56*, 8418–8426. [[CrossRef](#)]
70. Pietta, P.G. Flavonoids as antioxidants. *J. Nat. Prod.* **2000**, *63*, 1035–1042. [[CrossRef](#)]
71. Heim, K.E.; Tagliaferro, A.R.; Bobilya, D.J. Flavonoid antioxidants: Chemistry, metabolism and structure-activity relationships. *J. Nutr. Biochem.* **2002**, *13*, 572–584. [[CrossRef](#)]
72. Albayrak, S.; Aksoy, A.; Sagdic, O.; Hamzaoglu, E. Compositions, antioxidant and antimicrobial activities of *Helichrysum* (*Asteraceae*) species collected from Turkey. *Food Chem.* **2010**, *119*, 114–122. [[CrossRef](#)]
73. Nyambe-Silavwe, H.; Villa-Rodriguez, J.A.; Ifie, I.; Holmes, M.; Aydin, E.; Jensen, J.M.; Williamson, G. Inhibition of human α -amylase by dietary polyphenols. *J. Funct. Foods* **2015**, *19*, 723–732. [[CrossRef](#)]